their constituent monoatomic metal ions by showing no appreciable reactivity toward alkanes, $LaFe^+$ is reasonably reactive with alkanes. Simple dehydrogenation predominates its reactions with alkanes, while alternative pathways are possible when such dehydrogenation is blocked. Neopentane, for example, reacts with $LaFe^+$ to give both methane elimination and 1,3-dehydrogenation product ions. Carbon–carbon cleavage is a dominant process in the reaction of $LaFe^+$ with cyclopropane, which has its origin in the large ring strain.

Generally two series of CID product ions are formed by CID on $LaFe^+$–alkene ions. One series of fragments retain the dimer center and predominates at lower energy, and the other series arising from loss of Fe atom predominates at higher energy and resembles the CID spectra of the analogous La^+ complex. While CID of all of the $LaFe^+$–alkene ions studied tends to give a wide variety of fragment ions, two fragments in particular appear quite frequently. Not surprisingly, one of these fragments is $LaFeC_6H_6^+$ because of the special stability of benzene. For example, coupling of the two ligands in reaction 28 and dehydrocyclization in reaction 37 to give $LaFeC_6H_6^+$ are both efficient processes. More surprising, however, is the frequency in which $LaFeC_4H_4^+$ is observed as a CID product. Although additional studies will be necessary to draw definitive conclusions, one interesting possibility is that the ion has a $LaFe^+$–cyclobutadiene structure. There currently exist ample examples where a transition metal center can greatly stabilize the otherwise elusive cyclobutadiene species.[41]

The reactivity of $LaFe^+$ with saturated hydrocarbons is in contrast to the lack of reactivity observed on previously studied metal dimer ions. Preliminary results from our laboratory, however, indicate that $RhFe^+$ and $RhCo^+$ also react with alkanes.[27] Because of the lack of a comprehensive understanding of the metal–metal interaction for even simple dinuclear transition metal dimer ions at this stage, rationalization of the reactivities in terms of metal–metal bonding and other factors is difficult, if not impossible. Understanding or predicting such reactivities will require more theoretical and experimental study in this field.

Acknowledgment is made to the Division of Chemical Sciences in the Office of Basic Energy Sciences in the U.S. Department of Energy (DE-AC02-80ER10689) for supporting this research and to the National Science Foundation (CHE-8310039) for continued support of the FTMS methodology.

Registry No. La^+, 14175-57-6; $Fe(CO)_5$, 13463-40-6; $LaFe^+$, 111496-23-2; methane, 74-82-8; ethane, 74-84-0; propane, 74-98-6; *n*-butane, 106-97-8; *n*-pentane, 109-66-0; *n*-hexane, 110-54-3; isobutane, 75-28-5; neopentane, 463-82-1; 2,3-dimethylbutane, 79-29-8; cyclopropane, 75-19-4; cyclobutane, 287-23-0; cyclopentane, 287-92-3; cyclohexane, 110-82-7; methylcyclohexane, 108-87-2.

(40) Buckner, S. W.; Freiser, B. S., paper in preparation.

(41) Efraty, A. *Chem. Rev.* **1977**, *77*, 691.

Interaction of Adenosine 5′-Triphosphate with Mg^{2+}: Vibrational Study of Coordination Sites by Use of ^{18}O-Labeled Triphosphates

Hideo Takeuchi, Hiroshi Murata,† and Issei Harada*

Contribution from the Pharmaceutical Institute, Tohoku University, Aobayama, Sendai 980, Japan. *Received May 28, 1987*

Abstract: Infrared and Raman spectra were measured of ATP and its three isotopomers whose triphosphate oxygen atoms were selectively substituted by ^{18}O. The observed frequency shifts on ^{18}O-substitution made it possible to determine the contributions of each phosphate group (α, β, or γ) to the infrared and Raman bands. Several infrared bands of ATP or ^{18}O-labeled ATP were found to be assignable to vibrations predominantly involving one of the three phosphate groups. Frequency shifts of such localized vibrations on complex formation are useful to investigate the sites of coordination of Mg^{2+} to ATP. At pH 3.0, comparable frequency shifts were observed for the vibrations localized at individual PO_2^- groups together with intensity changes of main chain vibrations attributable to conformational isomerization in some of the ATP molecules. These infrared data can be interpreted as due to coexistence of α,β-, β,γ-, and α,γ-bidentates. At pH 7.5, an α-PO_2^- vibration shifted by the same frequency as that at pH 3.0, whereas β-PO_2^- vibrations showed twice as large shifts as those at pH 3.0. A similarly strong interaction of Mg^{2+} with γ-PO_3^{2-} was also suggested by the frequency shift data. MgATP at pH 7.5 is, thus, supposed to be a mixture of β,γ-bidentate and α,β,γ-tridentate complexes. Implications of the present findings for enzymatic reactions involving MgATP are discussed.

Adenosine 5′-triphosphate (ATP) is an energy transfer agent in biological systems, and the enzymatic reactions involving ATP usually require divalent cations, most often Mg^{2+}, as cofactors. Because of the relatively high concentration of Mg^{2+} in living cells and the high affinity of ATP for the cation, ATP largely exists as the 1:1 MgATP complex,[1] and such complexes are real substrates of some enzymatic reactions.[2]

Interactions of ATP with Mg^{2+} in aqueous solution have been studied intensively by spectroscopic methods, which have commonly shown that the adenine ring of ATP is not, or only negligibly, involved in the interactions with Mg^{2+}, but the triphosphate moiety interacts with the cation.[3-5] However, there is no agreement about which of the three phosphate groups (α, β, and γ) is involved in the Mg^{2+} coordination. ^{31}P NMR studies proposed several models for MgATP: β-monodentate,[6] β,γ-biden-

† Present address: Analytical Center, Research Institute, Chugai Pharmaceutical Co. Ltd., Takada 3-41-8, Toshima, Tokyo 171, Japan.

(1) Frey, C. M.; Stuehr, J. E. *J. Am. Chem. Soc.* **1972**, *94*, 8898-8904.
(2) Cleland, W. W. *Annu. Rev. Biochem.* **1967**, *36*, 77-112.
(3) Cohn, M.; Hughes, T. R., Jr. *J. Biol. Chem.* **1962**, *237*, 176-181.
(4) Happe, A. J.; Morales, M. *J. Am. Chem. Soc.* **1966**, *88*, 2077-2078.
(5) Lanir, A.; Yu, N. T. *J. Biol. Chem.* **1979**, *254*, 5882-5887.
(6) Tran-Dinh, S.; Roux, M.; Ellenberger, M. *Nucleic Acids Res.* **1975**, *2*, 1101-1110.

0002-7863/88/1510-0392$01.50/0

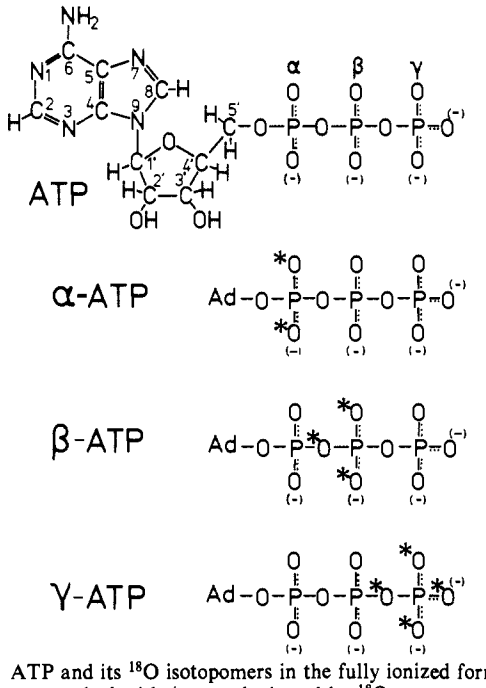

Figure 1. ATP and its ^{18}O isotopomers in the fully ionized form. The oxygen atoms marked with * are substituted by ^{18}O.

tate,[3,7] α,β,γ-tridentate,[8] and a mixture of α,β-, β,γ-, and α,γ-bidentates.[9] From broadening of ^{17}O NMR signals of ^{17}O-labeled ATP, Huang and Tsai concluded that all the α-, β-, and γ-phosphates interact with Mg^{2+} and the extent of α coordination is smaller than the β and γ coordination.[10]

The sites of coordination have been investigated also by infrared and Raman spectroscopy. From the infrared spectra at pH 8.9, Brintzinger proposed an equilibrating mixture of two complex forms, in which a Mg^{2+} ion interacts with one of the β- and γ-phosphates directly and with the other through a bridging water molecule.[11] A Raman spectroscopic study by Lewis et al. suggested a complex of Mg^{2+} binding to the α- and β-phosphates as an intermediate of a phosphate transfer reaction in dimethyl sulfoxide.[12] Those previous models for MgATP, however, do not seem conclusive because the contributions from the three phosphate groups to the infrared and Raman bands had not been fully clarified.

In this study, we prepared three isotopomers of ATP, [α-$^{18}O_2$]ATP (α-ATP), [$\alpha\beta$-^{18}O,β-$^{18}O_2$]ATP (β-ATP), and [$\beta\gamma$-^{18}O,γ-$^{18}O_3$]ATP (γ-ATP), shown in Figure 1. Measurements of infrared and Raman spectra of these isotopomers as well as unlabeled ATP and their Mg^{2+} complexes were made at pH 3.0 and 7.5, where the ionization state of the nucleotide is not affected by the complexation.[13] The isotopic substitution caused splitting of overlapped bands and enabled us to find several bands due to vibrations predominantly involving one of three phosphate groups. From the frequency shifts of such localized vibrations upon complexation with Mg^{2+}, we will discuss the coordination sites of Mg^{2+} to ATP.

Experimental Section

Materials. ATP was purchased from Kojin Chemical Co. and used without further purification. Chemical synthesis methods reported in the literature were used for the preparation of ^{18}O-labeled nucleotides. γ-ATP was obtained following the method of Webb.[14] Briefly, adenosine 5'-diphosphate was activated with carbonyldiimidazole and then coupled with the tri-*n*-butylammonium salt of [$^{18}O_4$]phosphate, which was prepared according to the method of Lowe and Sproat[15] from PCl_5 and 97%-enriched $H_2{}^{18}O$ (MSD, Merck). The ATP was purified on a column of DEAE-cellulose and identified by thin-layer chromatography on PEI-cellulose sheets.[16] Similar phosphorylation and purification methods were applied to the synthesis of β- and α-ATP. Adenosine 5'-[$\alpha\beta$-^{18}O,β-$^{18}O_3$]diphosphate, prepared using the method of Hassett et al.,[17] was activated with carbonyldiimidazole and then made to react with unlabeled tri-*n*-butylammonium phosphate to obtain β-ATP. α-ATP was synthesized by coupling of tri-*n*-butylammonium pyrophosphate[18] with the activated form of adenosine 5'-monophosphate-$^{18}O_3$, which was prepared following the procedure of Goody.[19] The tetrakis(triethylammonium) salts of all the ^{18}O-labeled ATP were finally converted to the tetrasodium salts with an excess of sodium iodide in acetone.[20]

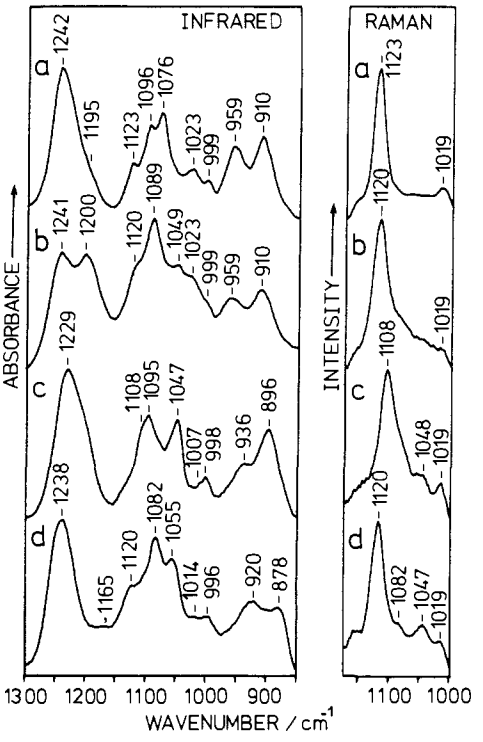

Figure 2. Infrared and Raman spectra of ATP and ^{18}O-labeled ATP at pH 3.0: (a) ATP, (b) α-ATP, (c) β-ATP, (d) γ-ATP.

Infrared Spectra. H_2O and D_2O were used as the solvents for recording infrared spectra in frequency regions of 1500–900 and 1150–700 cm^{-1}, respectively. The concentration of ATP (labeled or unlabeled) was 200 mM and the pH (pD) was adjusted with concentrated aqueous HCl (DCl) and NaOH (NaOD) to 3.0 or 7.5. (The pD values represent the direct reading on a pH meter.) For the MgATP 1:1 complex, a small excess of H_2O (D_2O) solution of $MgCl_2$ (4 M) was added to the ATP solution. The solution of ATP or MgATP was held between two ZnSe plates and the thickness of the sample was 15–20 μm. Infrared spectra were recorded on a JASCO IR-810 infrared spectrophotometer controlled by a microcomputer, and the background absorption due to the solvent was subtracted from the solution spectra. The wavenumber axis was calibrated for indene and gaseous ammonia, which gave an accuracy of ± 1 cm^{-1} for the peak frequencies of sharp bands. Infrared spectra of adenosine 5'-diphosphate (ADP) and MgADP were also measured in a similar way.

Raman Spectra. A JASCO CT-80D double monochromator equipped with a multichannel detection system (SMA, Princeton Instruments) was used to record Raman sectra of the H_2O solutions (100 mM) of ATP, ADP, and their Mg^{2+} complexes. The excitation wavelength was 488.0 nm of an Ar^+ laser. Frequency calibration of the Raman spectrometer was made with indene. Since some of the synthesized ATP samples contained fluorescent impurities, prolonged irradiation with the laser light in a cooled spinning cell was employed to reduce the fluorescence background.

(7) Terada, H.; Ikuno, M.; Shinohara, Y.; Yoshikawa, K. *Biochem. Biophys. Acta* **1984**, *767*, 648–650.
(8) Bishop, E. O.; Kimber S. J.; Orchard, D.; Smith, B. E. *Biochim. Biophys. Acta* **1981**, *635*, 63–72.
(9) Ramirez, F.; Marecek, J. F. *Biochem. Biophys. Acta* **1980**, 589, 21–29.
(10) Huang, S. L.; Tsai, M.-D. *Biochemistry* **1982**, *21*, 951–959.
(11) Brintzinger, H. *Biochim. Biophys. Acta* **1963**, *77*, 343–345.
(12) Lewis, A.; Nelson, N.; Racker, E. *Biochemistry* **1975**, *14*, 1532–1535.
(13) Heyde, M. E.; Rimai, L. *Biochemistry* **1971**, *10*, 1121–1128.
(14) Webb, M. R. *Biochemistry* **1980**, *19*, 4744–4748.
(15) Lowe, G.; Sproat, B. S. *J. Chem. Soc., Perkin Trans. 1* **1978**, 1622–1630.
(16) Eckstein, F.; Goody, R. S. *Biochemistry* **1976**, *15*, 1685–1691.
(17) Hassett, A.; Blättler, W.; Knowles, J. R. *Biochemistry* **1982**, *21*, 6335–6340.
(18) Hoard, D. E.; Ott, D. G. *J. Am. Chem. Soc.* **1965**, *87*, 1785–1788.
(19) Goody, R. S. *Anal. Biochem.* **1982**, *119*, 322–324.
(20) Murray, A. W.; Atkinson, M. R. *Biochemistry* **1968**, *11*, 4023–4029.

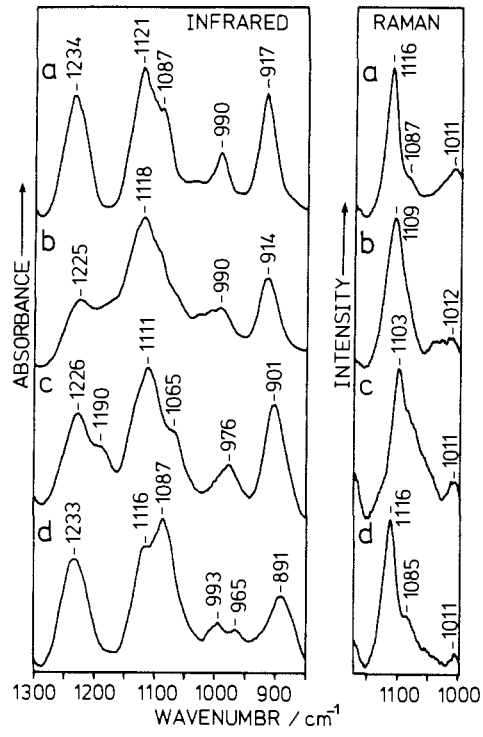

Figure 3. Infrared and Raman spectra of ATP and ^{18}O-labeled ATP at pH 7.5: (a) ATP, (b) α-ATP, (c) β-ATP, (d) γ-ATP.

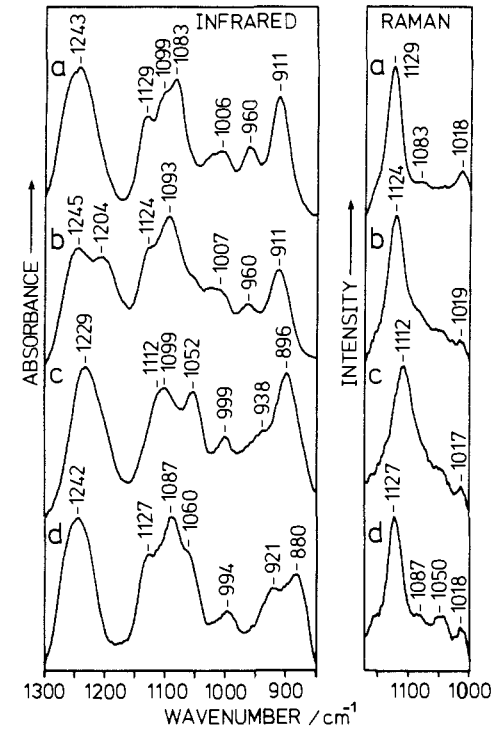

Figure 4. Infrared and Raman spectra of Mg^{2+} complexes with ATP and ^{18}O-labeled ATP at pH 3.0: (a) ATP, (b) α-ATP, (c) β-ATP, (d) γ-ATP.

Results

The S/N ratio of the infrared spectra was not satisfactory below 950 cm^{-1} for the H_2O solution and above 1100 cm^{-1} for the D_2O solution because of the strong absorption due to the solvent. In the common frequency region (1100–950 cm^{-1}) of both solution spectra, each sample showed no significant differences except the appearance of a weak band around 1030 cm^{-1} due to deuterated ribose[21,22] in the D_2O solution spectrum. For the simplicity of presentation, the H_2O and D_2O solution spectra of each sample were merged into a spectrum by using the absorption bands between 1000 and 950 cm^{-1} as the intensity standard. Thus the infrared spectra to be shown represent the H_2O and D_2O solution spectra above and below 950 cm^{-1}, respectively.

Figures 2 and 3 show the effects of ^{18}O-substitution on the infrared and Raman spectra of ATP at pH 3.0 and 7.5, respectively. Most of the bands in the frequency regions shown shift in frequency on ^{18}O-substitution, and it is seen that vibrations of the triphosphate moiety appear intensively compared with those of the adenine and ribose moieties.

Infrared and Raman spectra of 1:1 mixtures of ATP and Mg^{2+} at pH 3.0 and 7.5 are shown in Figures 4 and 5, respectively. The pH values and the concentrations of ATP and Mg^{2+} adopted here ensure that ATP molecules form 1:1 complexes predominantly[23] and the ionization state does not change on complexation.[13] Significant frequency shifts (>2 cm^{-1}) on complexation are evident for some infrared and Raman bands. Slight band broadening is also observed for many bands, and large changes in intensity are noted for the infrared bands below 970 cm^{-1} at pH 3.0.

Discussion

Assignments of Infrared and Raman Bands at pH 3.0. The N_1 atom of the adenine ring and one oxygen atom of the γ-phosphate are protonated at this pH value. The triphosphate chain is, therefore, composed of three PO_2^- groups with six P–O single bonds of the main chain and one O–H bond at the terminal phosphate.

Antisymmetric stretching vibrations [$\nu_a(PO_2^-)$] of the three PO_2^- groups are expected in the 1250–1150-cm^{-1} region.[24] The

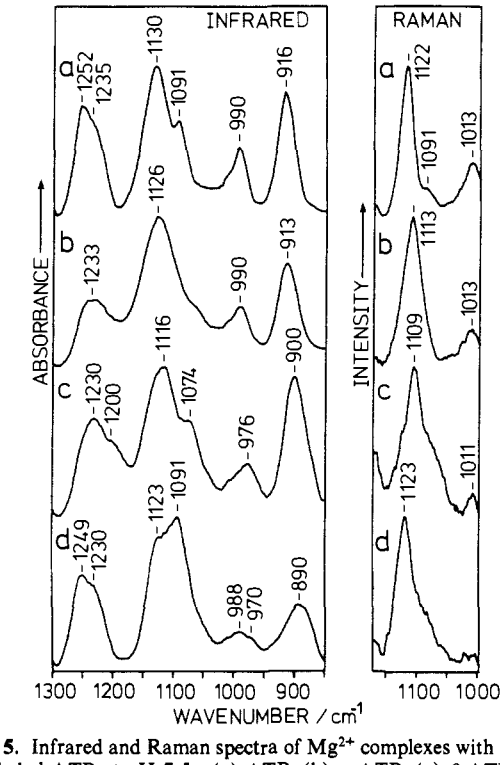

Figure 5. Infrared and Raman spectra of Mg^{2+} complexes with ATP and ^{18}O-labeled ATP at pH 7.5: (a) ATP, (b) α-ATP, (c) β-ATP, (d) γ-ATP.

infrared spectrum of ATP shows a broad absorption band peaked at 1242 cm^{-1} with a shoulder around 1195 cm^{-1} (see Figure 2). On ^{18}O-substitution at the γ position, the shoulder shifts down to ~1165 cm^{-1} leaving a sharper band centered at 1238 cm^{-1} (this shift was confirmed by a difference spectrum). The 1195- and 1165-cm^{-1} vibrations are thus assigned to $\nu_a(\gamma\text{-}PO_2^-)$ and $\nu_a(\gamma\text{-}P^{18}O_2^-)$, respectively, and the 1242- and 1238-cm^{-1} bands are ascribed to an overlap of $\nu_a(\alpha\text{-}PO_2^-)$ and $\nu_a(\beta\text{-}PO_2^-)$. ^{18}O-Substitution at the α position splits the 1242-cm^{-1} band into two bands at 1241 and 1200 cm^{-1}. The virtually unshifted component at

(21) Tsuboi, M. *Appl. Spectrosc. Rev.* **1969**, *3*, 45–90.
(22) Khalil, F.; Brown, T. L. *J. Am. Chem. Soc.* **1964**, *86*, 5113–5117.
(23) Phillips, R. *Chem. Rev.* **1966**, *66*, 501–527.

1241 cm^{-1} is assigned to $\nu_a(\beta\text{-}PO_2^-)$ and the shifted 1200 cm^{-1} component to $\nu_a(\alpha\text{-}P^{18}O_2^-)$ overlapping a weaker band around 1195 cm^{-1} due to $\nu_a(\gamma\text{-}PO_2^-)$. In contrast to the spectrum of α-ATP, no splitting is observed in the spectrum of β-ATP, which shows a broad band peaked at 1229 cm^{-1} and tailing to the low-frequency side. The difference in the effects of α- and β-substitution is accounted for by assuming that the frequency of $\nu_a(\alpha\text{-}PO_2^-)$ is about 10 cm^{-1} lower than that of $\nu_a(\beta\text{-}PO_2^-)$, and the separation in frequency becomes large enough to give a doublet in α-ATP but remains too small to split the band in β-ATP.

The PO_2^- symmetric stretching vibrations $[\nu_s(PO_2^-)]$ are expected around 1100 cm^{-1}.[24] Three infrared bands of unlabeled ATP at 1123, 1096, and 1076 cm^{-1} and a strong Raman band at 1123 cm^{-1} are assigned to these vibrations. The appearance of a single strong and sharp band in the Raman spectrum suggests considerable mixing of the $\nu_s(PO_2^-)$ vibrations among the three phosphate groups. Namely, the 1123-cm^{-1} vibration, strong in the Raman spectrum and weak in the infrared spectrum, is assigned to an in-phase mode of three PO_2^- groups, and the other two appearing at 1096 and 1076 cm^{-1} in the infrared spectrum are assigned to out-of-phase modes. The distinction between the in-phase and out-of-phase modes holds in the labeled ATP, and the in-phase mode is observed with high Raman and low infrared intensities at 1120, 1108, and 1120 cm^{-1} for α-, β-, and γ-ATP, respectively. On the other hand, two out-of-phase vibrations show drastic changes in the infrared intensity distribution upon ^{18}O-substitution, presumably because of changes in the mode mixing pattern. The lower frequency component at 1049 (α-ATP), 1047 (β-ATP), or 1055 cm^{-1} (γ-ATP) is very likely to involve the ^{18}O-substituted phosphate group predominantly.

Frequency shifts on ^{18}O-substitution are also observed below 1050 cm^{-1}. Two infrared bands at 959 and 910 cm^{-1} in the spectrum of ATP shift down to 936 and 896 cm^{-1} in β-ATP and to 920 and 878 cm^{-1} in γ-ATP, respectively. These infrared bands are assigned to P–O stretching vibrations, ν(P–O), of the main chain. In β- and γ-ATP, at least one of the oxygen atoms of the six P–O single bonds is substituted by ^{18}O (see Figure 1) and the ν(P–O) vibrations show frequency downshifts. In α-ATP, on the other hand, no oxygen atoms of the P–O bonds are replaced by ^{18}O, and consistently no frequency shifts are seen for the ν(P–O) bands. A similar pattern of frequency shift is observed for a weak infrared band at 1023 cm^{-1} of ATP, which shifts to 1007 and 1014 cm^{-1} in β- and γ-ATP, respectively. Accordingly, this band is assigned to another ν(P–O) vibration. The 999-cm^{-1} infrared band of ATP does not show a large shift on ^{18}O-substitution at any phosphate group and may be assigned to a stretching vibration of the C_5'–O–P_α likage. A weak Raman band at 1019 cm^{-1} is ascribed to the adenine ring.[25]

Assignments of Infrared and Raman Bands at pH 7.0. The N_1 atom of the adenine ring and the γ-phosphate group are deprotonated at this pH value. Thus the triphosphate chain is composed of two PO_2^- groups at α and β positions and one PO_3^{2-} group at the γ position.

A broad infrared band due to $\nu_a(\alpha\text{-}PO_2^-)$ and $\nu_a(\beta\text{-}PO_2^-)$ appears at 1234 cm^{-1} in ATP (see Figure 3). The peak frequency probably represents an average of those of the two overlapping components. In α-ATP, $\nu_a(\beta\text{-}PO_2^-)$ has a frequency of 1225 cm^{-1} and $\nu_a(\alpha\text{-}P^{18}O_2^-)$ is located around 1180 cm^{-1}. The infrared band due to the latter vibration fills in the valley between the $\nu_a(PO_2^-)$ and $\nu_s(PO_2^-)$ regions and hence the peak position is unclear. Two infrared bands of β-ATP at 1226 and 1190 cm^{-1} are assigned to $\nu_a(\alpha\text{-}PO_2^-)$ and $\nu_a(\beta\text{-}P^{18}O_2^-)$, respectively. The spectrum of γ-ATP in the $\nu_a(PO_2^-)$ region is substantially the same as that of unlabeled ATP as expected.

The degenerate stretching vibration of the terminal PO_3^{2-} group, $\nu_d(\gamma\text{-}PO_3^{2-})$, is expected in a frequency region of 1120–1070 cm^{-1},[24] which overlaps that of the $\nu_s(PO_2^-)$ vibrations of α- and β-phosphates. Such overlap may result in coupling between the two vibrational modes. However, the coupling is negligible between $\nu_d(\gamma\text{-}PO_3^{2-})$ and the in-phase $\nu_s(PO_2^-)$ mode because a strong and sharp Raman band assignable to the in-phase mode is observed at 1116 cm^{-1} for ATP as well as for γ-ATP. The corresponding Raman band is seen at 1109 cm^{-1} in α-ATP with a slightly broader band shape and at 1103 cm^{-1} in β-ATP as an asymmetric band tailing to the low frequency side. The tailing implies significant changes in mode distribution as a result of the β-^{18}O-substitution. A weak Raman band of ATP observed at 1087 cm^{-1} is assigned to the out-of-phase $\nu_s(PO_2^-)$ mode, which is also observed as a shoulder peak in the infrared spectrum. Since the out-of-phase mode is weak in both infrared and Raman spectra, its isotopic shift is not evident except for β-ATP, a shoulder of which observed at 1065 cm^{-1} is attributable to this mode mainly involving the vibration at the β-phosphate. The strong 1121-cm^{-1} infrared band of ATP is assigned to $\nu_d(\gamma\text{-}PO_3^{2-})$ overlapping a weaker absorption at 1116 cm^{-1} due to the in-phase $\nu_s(PO_2^-)$ mode. The $\nu_d(\gamma\text{-}PO_3^{2-})$ band shifts to 1118 cm^{-1} in α-ATP and to 1111 cm^{-1} in β-ATP due to coupling with the out-of-phase $\nu_s(PO_2^-)$ vibrations, the coupling being weak with $\alpha\text{-}PO_2^-$ and strong with $\beta\text{-}PO_2^-$. A prominent infrared band at 1087 cm^{-1} of γ-ATP is attributable to $\nu_d(\gamma\text{-}P^{18}O_3^{2-})$ coupled with the out-of-phase mode of $\nu_s(\alpha\text{-}PO_2^-)$ and $\nu_s(\beta\text{-}PO_2^-)$.

Two ν(P–O) vibrations appear at 990 and 917 cm^{-1} in the infrared spectrum of ATP. The 990-cm^{-1} band shifts down to 976 cm^{-1} in β-ATP, while it is almost unshifted in γ-ATP. Accordingly this band is assigned to ν(P–O) of the P_α–O–P_β linkage. On the other hand, the 917-cm^{-1} band of ATP shows the largest downshift on γ-substitution and is assigned to a ν(P–O) vibration primarily involving the P_β–O–P_γ linkage. In addition to the ν(P–O) bands, a new band is observed at 965 cm^{-1} for γ-ATP. We assign this band to the symmetric stretching vibration of the $\gamma\text{-}PO_3^{2-}$ group, $\nu_s(\gamma\text{-}P^{18}O_3^{2-})$. The counterpart infrared band due to $\nu_s(\gamma\text{-}P^{16}O_3^{2-})$ in ATP, α-ATP, and β-ATP may be located around 1000 cm^{-1} and covered by the stronger ν(P–O) band around 990 cm^{-1}. The Raman band around 1010 cm^{-1} is due to an adenine ring vibration,[25] being superimposed on the $\nu_s(PO_3^{2-})$ band in unlabeled ATP, α-ATP, and β-ATP.

Effects of Mg^{2+}. At both pH 3.0 and 7.5, Mg^{2+} binding causes significant frequency upshifts of $\nu_a(PO_2^-)$, $\nu_s(PO_2^-)$, $\nu_a(PO_3^{2-})$, and $\nu_s(PO_3^{2-})$ bands, whereas the frequencies of ν(P–O) bands are hardly affected by the cation (see Figures 4 and 5). Of the shifted bands, ones due to vibrations localized at one phosphate group are of particular interest, because frequency shifts of such vibrations enable us to specify the sites of coordination. On the other hand, delocalized vibrations, e.g., the in-phase $\nu_s(PO_2^-)$ mode giving rise to a strong Raman band, may undergo variation in mode distribution and could not reflect the local perturbation by Mg^{2+} in a simple manner. Table I lists the frequency shifts on complexation for the infrared bands that have been assigned to localized or nearly localized vibrations.

At pH 3.0, binding of Mg^{2+} causes a frequency shift of $\nu_a(\beta\text{-}PO_2^-)$ of α-ATP from 1241 to 1245 cm^{-1}. The $\nu_s(\beta\text{-}P^{18}O_2^-)$ band

Table I. Localized Vibrations and Their Frequency Shifts on Complexation with Mg^{2+}

compound	frequency[a]	assignment	shift[a]
	pH 3.0		
α-ATP	1241	$\nu_a(\beta\text{-}PO_2^-)$	4
	1200	$\nu_a(\alpha\text{-}P^{18}O_2^-)$	4
β-ATP	1047	$\nu_s(\beta\text{-}P^{18}O_2^-)$	5
γ-ATP	1055	$\nu_s(\gamma\text{-}P^{18}O_2^-)$	5
	pH 7.5		
ATP	1121	$\nu_d(\gamma\text{-}PO_3^{2-})$	9
α-ATP	1225	$\nu_a(\beta\text{-}PO_2^-)$	8
	1118	$\nu_d(\gamma\text{-}PO_3^{2-})$	8
β-ATP	1226	$\nu_a(\alpha\text{-}PO_2^-)$	4
	1190	$\nu_a(\beta\text{-}P^{18}O_2^-)$	10
	1065	$\nu_s(\beta\text{-}PO_2^-)$	9
γ-ATP	965	$\nu_s(\gamma\text{-}P^{18}O_3^{2-})$	5

[a] In units of cm^{-1}.

(24) Shimanouchi, T.; Tsuboi, M.; Kyogoku, Y. *Adv. Chem. Phys.* **1964**, *7*, 435–498.

(25) Lord, R. C.; Thomas, G. J., Jr. *Spectrochim. Acta, Part A* **1967**, *23*, 2551–2591.

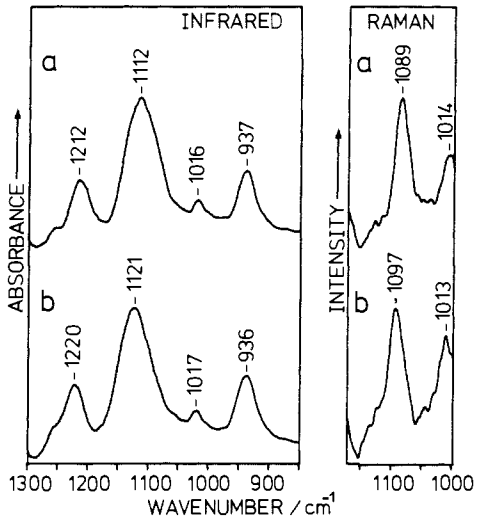

Figure 6. Effects of Mg^{2+} on the infrared and Raman spectra of ADP at pH 7.5: (a) ADP, (b) MgADP. Infrared bands of ADP at 1212 and 1112 cm^{-1} are due to $\nu_a(\alpha\text{-}PO_2^-)$ and $\nu_d(\beta\text{-}PO_3^{2-})$, respectively. A Raman band at 1089 cm^{-1} is assigned to $\nu_s(\alpha\text{-}PO_2^-)$, which is weak in the infrared spectrum and covered by the strong $\nu_d(\beta\text{-}PO_3^{2-})$ band.

of β-ATP is also upshifted from 1047 to 1052 cm^{-1}. These two shifts show that Mg^{2+} interacts with $\beta\text{-}PO_2^-$. A frequency shift of 4 cm^{-1} observed for the 1200-cm^{-1} band of α-ATP, $\nu_a(\alpha\text{-}P^{18}O_2^-)$, is indicative of interaction with the α-phosphate. Evidence for the coordination to the γ-phosphate is given by an upshift of 5 cm^{-1} of the $\nu_s(\gamma\text{-}P^{18}O_2^-)$ band in γ-ATP from 1055 to 1060 cm^{-1}. In addition to these shifts, the 959-cm^{-1} ν(P–O) band of ATP decreases in intensity on complexation and concomitantly the 910 cm^{-1} ν(P–O) band gains intensity. Similar intensity changes are also apparent for the corresponding ν(P–O) bands of ^{18}O-labeled ATP.

At pH 7.5, large frequency shifts due to Mg^{2+} binding are observed for the vibrations localized at $\beta\text{-}PO_2^-$. The 1225-cm^{-1} infrared band of α-ATP assigned to $\nu_a(\beta\text{-}PO_2^-)$ shifts up by 8 cm^{-1}. Of the vibrations of β-ATP, both $\nu_a(\beta\text{-}P^{18}O_2^-)$ (1190 cm^{-1}) and $\nu_s(\beta\text{-}P^{18}O_2^-)$ (1065 cm^{-1}) bands shows upshifts of 10 and 9 cm^{-1}, respectively. These provide direct evidence of the binding of Mg^{2+} to the β-phosphate. Similarly, a small shifts of 4 cm^{-1} observed for the $\nu_a(\alpha\text{-}PO_2^-)$ infrared band of β-ATP at 1226 cm^{-1} suggests the interaction with the α-phosphate. Evidence for the interaction with $\gamma\text{-}PO_3^{2-}$ is found in the infrared spectra as well. The $\nu_s(\gamma\text{-}P^{18}O_3^{2-})$ band of γ-ATP shifts from 965 to 970 cm^{-1}. Furthermore, the 1121- and 1118-cm^{-1} bands of ATP and α-ATP due to $\nu_d(\gamma\text{-}PO_3^{2-})$ shift up by 9 and 8 cm^{-1}, respectively. In contrast to the case of pH 3.0, marked intensity changes are not observed for the ν(P–O) bands at pH 7.5.

Structure of MgATP. The frequency shifts of localized vibrations summarized in Table I are useful in elucidating the structure of MgATP. From the table, it is obvious that $\nu_a(PO_2^-)$ and $\nu_s(PO_2^-)$ vibrations localized at a certain phosphate group are affected by Mg^{2+} to the same extent, and there is no difference between these two modes as far as the frequency shifts are concerned. The frequency shifts observed for the PO_2^- vibrations are classified into two groups, those at 4–5 cm^{-1} and others in a range of 8–10 cm^{-1}. The difference in frequency shift might be related to the strength of coordination. Another possibility is that a shift of 4–5 cm^{-1} represents an average value of a shift of 8–10 cm^{-1} and a null shift, which are respectively due to complex forms whose particular PO_2^- group is involved and not involved in the Mg^{2+} coordination. If the latter case is true the bandwidth is expected to increase on complexation. In fact, the infrared and Raman spectra show band broadening on complexation and suggest the coexistence of some complex forms at both pH 3.0 and 7.5. This interpretation is supported by the infrared and Raman spectra of ADP and MgADP shown in Figure 6. At pH 7.5, ADP contains one PO_2^- and one PO_3^{2-} group and Mg^{2+} is believed to bind to both phosphate groups in a bidentate manner.[3] The $\nu_a(PO_2^-)$ (1212 cm^{-1}), $\nu_s(PO_2^-)$ (1089 cm^{-1}), and $\nu_a(PO_3^{2-})$ (1112 cm^{-1}) bands of ADP shift by 8, 8, and 9 cm^{-1}, respectively, without broadening of the bands. Therefore, it is very likely that the smaller frequency shifts (4–5 cm^{-1}) and band broadening observed for some localized vibrations of ATP result from the coexistence of different complex forms, in one of which a particular PO_2^- group is bound to Mg^{2+} and in another the phosphate is not involved in the coordination. On this assumption, we will discuss the main structure of MgATP at pH 3.0 and 7.5.

The shifts observed at pH 3.0 are in a range of 4–5 cm^{-1} for all the vibrations localized at α-, β-, or $\gamma\text{-}PO_2^-$, and this finding suggests that the three PO_2^- groups interact with Mg^{2+} to the same extent as an average of some complex forms. A mixture of α,β-, β,γ-, and α,γ-bidentates is consistent with the infrared data. Another possibility is a mixture of α-, β-, and γ-monodentates. A support for the bidentate mixture is given by the intensity change of the ν(P–O) bands at 950 and 910 cm^{-1}. As described above, Mg^{2+} binding makes the 959-cm^{-1} band weaker and the 910-cm^{-1} band stronger. This intensity change amounts to about 30% and is attributable to conformational change of the triphosphate chain because binding of Mg^{2+} is unlikely to affect the intensities of ν(P–O) bands directly. The conformational isomerization is probably induced not by monodentate but by bidentate coordination, especially α,γ-bidentate which makes two distant phosphate groups close together. In the absence of Mg^{2+}, ATP may take two conformations giving rise to the 959- and 910-cm^{-1} bands, respectively. This assignment is consistent with a preliminary observation that the intensity ratio of the 959-cm^{-1} band to the 910-cm^{-1} band decreases at lower temperatures. In the presence of the cation, the conformer responsible for the 910-cm^{-1} band is able to form a stable α,γ-bidentate complex with Mg^{2+} without conformational change while the conformer giving the 959-cm^{-1} band is required to isomerize in order to bind to Mg^{2+} in the α,γ-bidentate manner.

Deprotonation at the γ-phosphate seems to affect the structure of the complex to be formed. The infrared spectra of MgATP at pH 7.5 are characterized by pronounced frequency shifts of the vibrations localized at $\beta\text{-}PO_2^-$. The shifts are almost the same as those observed for ADP and indicate that Mg^{2+} binds to the β-phosphate tightly. Similarly, the shift of $\nu_d(PO_3^{2-})$, which is also as large as that of ADP, suggests a stable binding of Mg^{2+} to $\gamma\text{-}PO_3^{2-}$. The smaller shift (5 cm^{-1}) of $\nu_s(\gamma\text{-}P^{18}O_3^{2-})$ may be accounted for by small displacements of the oxygen atoms in this mode compared with those in $\nu_d(PO_3^{2-})$. The frequency shift of $\nu_a(\alpha\text{-}PO_2^-)$ is 4 cm^{-1}, and this suggests the coexistence of complex forms coordinated and uncoordinated at the α-phosphate. We, therefore, conclude that MgATP at pH 7.5 is a mixture of β,γ-bidentate and α,β,γ-tridentate.

The present conclusion on the structure of MgATP at pH 7.5 is consistent with that reached by ^{17}O NMR analysis.[10] The coexistence of two complex forms in aqueous solution may be related to the mechanisms of enzymatic reactions involving MgATP. X-ray crystallographic studies of phosphoglycerate kinase suggested a β,γ-bidentate coordination in the active site of the enzyme, though the exact location of Mg^{2+} could not be determined.[26] In crystalline phosphofruktokinase, Mg^{2+} was found to bind to an ATP analogue (5′-adenylylimidodiphosphate) in a β,γ-bidentate manner.[27] Kinetic, CD, and radioisotopic assay studies on several kinases using isomerization-inert CrATP complexes instead of MgATP showed that the β,γ-bidentate and not α,β,γ-tridentate CrATP served as a substrate of the enzymes, even though the tridentate bound to some enzymes better than the bidentate.[28] These previous findings imply that the β,γ-bidentate MgATP is the active isomer in the enzyme and the α,β,γ-tridentate isomer can improve, in some cases, the total affinity of MgATP to the enzyme. Since these two isomers are expected

(26) Blake, C. C. F.; Rice, D. W. *Phil. Trans. R. Soc. London, Ser. A* **1981**, *293*, 93–104.
(27) Evans P. R.; Farrants, G. W.; Hudson P. J. *Phil. Trans. R. Soc. London, Ser. B* **1981**, *293*, 53–62.
(28) Dunaway-Mariano, D; Cleland, W. W. *Biochemistry* **1980**, *19*, 1506–1515.

to be easily convertible to each other under physiological conditions, their coexistence may be useful for MgATP to bind to a variety of ATP-utilizing enzymes and to become an active substrate without or through isomerization.

Conclusion

Vibrational spectroscopy in conjunction with ^{18}O isotopic substitution have been shown to be a useful method to reveal the sites of coordination of Mg^{2+} to ATP. From the isotopic frequency shifts, several infrared bands have been found to be due to vibrations localized or nearly localized at individual phosphate groups of the triphosphate. Frequency shifts on complexation with Mg^{2+} observed for such localized vibrations indicate that the MgATP complexes exist as a mixture of α,β-, β,γ-, and α,γ-bidentates when the γ-phosphate is protonated. At pH 7.5, where the γ-phosphate is not protonated, ATP forms β,γ-bidentate and α,β,γ-tridentate complexes with Mg^{2+}. The variety of MgATP complex forms may be related to the fact that various enzymes utilizing ATP require Mg^{2+} as cofactors.

Acknowledgment. We are grateful to Dr. M. Katagiri for valuable advice about the preparation of ^{18}O-labeled ATP. This work was supported by a Grant-in-Aid for Scientific Research No. 60740251 from the Ministry of Education, Science, and Culture.

Registry No. ATP, 56-65-5; α-ATP, 111616-21-8; β-ATP, 73135-75-8; γ-ATP, 73116-39-9; Mg^{2+}, 22537-22-0.

Active Oxygen on Group VIII Metals: Activation of Formic Acid and Formaldehyde on Pd(100)

Scott W. Jorgensen and R. J. Madix*

Contribution from the Department of Chemical Engineering, Stanford University, Stanford, California 94305. *Received June 12, 1987*

Abstract: The reactions of formic acid and formaldehyde were studied individually on the clean and oxygen-predosed Pd(100) surface by using temperature-programmed reaction and vibrational spectroscopies. On the clean surface formic acid partially decomposes to give CO, while formaldehyde dehydrogenates to CO and H_2. The formate species was identified on the oxygen-precovered surface in each case. This result clearly shows that the pattern of activation by oxygen via nucleophilic attack of electron-deficient centers or Brønsted basicity previously reported on copper, silver, and gold single-crystal surfaces is also exhibited on the group VIII metal palladium.

Direct activation by adsorbed oxygen plays a major role in the selective oxidation of alcohols,[1-3] nitriles,[4] and amines[5] on silver surfaces. In addition, it has been shown that C–H bonds in allyls or alkynes are activated in the same fashion.[6] These reactions indicate that the oxygen has an appreciable Brønsted basicity. Furthermore, the nucleophilicity of this type of oxygen has been established for oxidations of aldehydes and methyl formate.[3] Similar reactivity exists for oxygen on both copper[7] and gold surfaces,[8,9] so that these general patterns of reactivity appear well established for the group IB metals. The behavior of adsorbed oxygen on group VIII metals is, however, not yet well characterized. Brønsted basicity of adsorbed oxygen has been established on Pt(111)[10] and Pd(100)[11] for reaction with water to form hydroxyl groups. Similarly, the hydroxyl proton in methanol is transferred directly to surface oxygen on Pd(100).[12]

The oxidation reactions of formic acid and formaldehyde have been studied on several single-crystal surfaces[13-21] with a combination of temperature-programmed reaction and vibrational spectroscopies.[15-17] In these studies the formate intermediate has

Table I. Comparative Vibrational Frequencies (cm^{-1}) for HCOOH and H_2CO[a]

mode	Pd(100) HCOOH	Pd(100) D_2CO	Pt(111) HCOOH	Ag(110) H_2CO
δ(OCO)	700		715	
π(CH/CD)	1220	855	1235	1250 (935)
	1385	1090	1385	1490 (1115)
ν(CO)	950		970	
	1685	1635	1720	1710
ν(CH/CD)	2660	2195	2500	2850 (2135)
	3000		3050	
ν(OH)	3320		>3000	

[a] All spectra taken at 80 K and 1–2 eV beam energy. The values in parentheses are estimates of the CD frequencies for D_2CO based on the data from ref 17.

Chart I

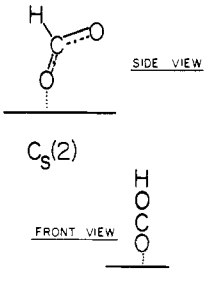

(1) Madix, R. J. *Science* **1986**, *223*, 1159.
(2) Bowker, M.; Barteau, M. A.; Madix, R. J. *Surf. Sci.* **1980**, *92*, 528.
(3) Barteau, M. A.; Bowker, M.; Madix, R. J. *Surf. Sci.* **1980**, *94*, 303.
(4) Capote, A. J.; Hamza, A. V.; Canning, N. D. S.; Madix, R. J. *Surf. Sci.* **1986**, *175*, 445.
(5) Madix, R. J.; Thornburg, M., to be published.
(6) Barteau, M. A.; Madix, R. J. *Surf. Sci.* **1982**, *115*, 355.
(7) Bowker, M.; Madix, R. J. *J. Electron Spectrosc. Relat. Phenom.* **1980**, *20*, 281.
(8) Outka, D. A.; Madix, R. J. *Surf. Sci.* **1987**, *279*, 361.
(9) Outka, D. A.; Madix, R. J. *J. Am. Chem. Soc.* **1987**, *109*, 1708.
(10) Fisher, G. B.; Gland, J. L. *Surf. Sci.* **1980**, *94*, 446.
(11) Stuve, E. M.; Jorgensen, S. W. Madix, R. J. *Surf. Sci.* **1984**, *146*, 179.
(12) Jorgensen, S. W.; Madix, R. J. *Surf. Sci.* **1987**, *179*, 1.
(13) Wachs, I. E.; Madix, R. J. *Surf. Sci.* **1979**, *84*, 375.
(14) Barteau, M. A.; Bowker, M.; Madix, R. J. *Surf. Sci.* **1980**, *94*, 303.
(15) Avery, N. R. *Appl. Surf. Sci.* **1983**, *14*, 149.
(16) Sexton, B. A. *Surf. Sci.* **1979**, *88*, 319.
(17) Stuve, E. M.; Madix, R. J.; Sexton, B. A. *Surf. Sci.* **1982**, *119*, 279.
(18) Sexton, B. A.; Madix, R. J. *Surf. Sci.* **1981**, *105*, 177.
(19) Gdowski, G. E.; Fair, J. A.; Madix, R. J. *Surf. Sci.* **1983**, *127*, 541.

0002-7863/88/1510-0397$01.50/0